Arterial waves in humans during peripheral vascular surgery

Ashraf W. KHIR*, Michael Y. HENEIN†, Tat KOH†, Saroj K. DAS‡, Kim H. PARKER* and Derek G. GIBSON†

*Physiological Flow Study Group, Department of Bioengineering, Imperial College of Science, Technology and Medicine, Prince Consort Rd., London SW7 2BY, U.K., †Echocardiography Department, Royal Brompton Hospital, Sydney St., London SW3 6NP, U.K., and ‡Vascular Surgery Department, Hillingdon Hospital, Pield Heath Road, Hillingdon, Uxbridge, Middlesex UB8 3NN, U.K.

A B S T R A C T

The purpose of this study was to investigate the effect of aortic clamping on arterial waves during peripheral vascular surgery. We measured pressure and velocity simultaneously in the ascending aorta, in ten patients (70 ± 5 years) with aortic-iliac disease intra-operatively. Pressure was measured using a catheter tip manometer, and velocity was measured using Doppler ultrasound. Data were collected before aortic clamping, during aortic clamping and after unclamping. Hydraulic work in the aortic root was calculated from the measured data, the reflected waves were determined by wave-intensity analysis and wave speed was determined by the PU-loop (pressure–velocity-loop) method; a new technique based on the 'water-hammer' equation. The wave speed is approx. 32% ($P < 0.05$) higher during clamping than before clamping. Although the peak intensity of the reflected wave does not alter with clamping, it arrives 30 ms ($P < 0.05$) earlier and its duration is 25% ($P < 0.05$) longer than before clamping. During clamping, left ventricule (LV) hydraulic systolic work and the energy carried by the reflected wave increased by 27% ($P < 0.05$) and 20% ($P < 0.05$) respectively, compared with before clamping. The higher wave speed during clamping explains the earlier arrival of the reflected waves suggesting an increase in the afterload, since the LV has to overcome earlier reflected compression waves. The longer duration of the reflected wave during clamping is associated with an increase in the total energy carried by the wave, which causes an increase in hydraulic work. Increased hydraulic work during clamping may increase LV oxygen consumption, provoke myocardial ischaemia and hence contribute to the intra-operative impairment of LV function known in patients with peripheral vascular disease.

INTRODUCTION

Peripheral and coronary artery disease often occur together. Peripheral arterial reconstruction surgery in the presence of concurrent left ventricle (LV) disease, a common sequela of long-standing coronary artery disease, may increase peri-operative mortality and morbidity. The rate of mortality during the 30 day period following thoraco-abdominal aneurysm repair ranges from 8% to 35% [1–3]. The mortality and morbidity rate during and immediately following vascular surgery is approx. 10% [4], half of which is due to myocardial infarction [5]. We have suggested previously that aortic clamping may impair subendocardial function in such patients [6]. LV function, as indicated by long-axis shortening fraction, deteriorates during the operation, recovers a few minutes after the release of the clamp and becomes normal within 5 days of surgery. The mechanism underlying this behaviour has not yet been established. We hypothesize that during clamping there

Key words: aortic clamping, haemodynamics, reflected waves, wave intensity.

Abbreviations: LV, left ventricle; PU-loop, pressure–velocity loop.

Correspondence: Dr Ashraf Khir (e-mail a.khir@ic.ac.uk).

is an increase in the energy carried by the reflected waves. These enlarged reflected waves could cause an increase in LV hydraulic work and alter afterload, which could provide an explanation to the deterioration in LV function seen in humans during aortic clamping [6].

METHODS

This study was carried out on ten patients (eight males), age 70±5 years, who were undergoing peripheral vascular reconstruction surgery. All patients had a documented history of stable coronary artery disease, and none had an acute or unstable event for more than 6 months prior to surgery. Pre-operative echocardiography assessment confirmed that no patient had structural valve disease, and that all patients, except two, had a normal ejection fraction. The clamping site for all the patients was distal to the level of the renal arteries in the abdominal aorta. The patients were studied in the operating theatre under general anaesthesia. The protocol of this study was approved by the Ethics Committee of the Royal Brompton Hospital, and written informed consent was obtained from all patients prior to surgery.

All patients were operated on under general anaesthesia after premedication with temazepam. They were induced with 10 μg/kg fentanyl and 0.1–0.2 mg/kg etomidate, paralysed with pancuronium 0.1 mg/kg and maintained on isoflurane, O_2 and NO. Blood pressure was controlled with glyceryl trinitrate.

Aortic root pressure and velocities were recorded at three stages during the operation: before, during clamping and after unclamping. Recordings were made at several different times during clamping in three of the patients. All operations were carried out by a single vascular surgeon, and data were collected by the same cardiologist.

In order to apply wave-intensity analysis, it is vital that aortic pressure and velocities are measured simultaneously and at the same site. We measured pressure and velocities in the ascending aorta, just distal to the aortic valve. The pressure catheter (6F; Millar Instruments, Houston, TX, U.S.A.) was inserted through a sheath in the right femoral artery of the patient and advanced under fluroscope observation until it reached the measurement site in the ascending aorta. The catheter has an upper frequency limit of 2 kHz. Aortic velocities were measured by Doppler ultrasound echocardiograph (Sonos 500, Hewlett–Packard) using an imaging transducer with a frequency of 2.5 kHz. Eight patients were studied using trans-oesophageal imaging and two, in whom this was technically difficult, were studied using the trans-thoracic approach.

The lack of analogue-to-digital conversion in the operating theatre dictated the method of collecting the data. Aortic pressures, velocities and ECG were recorded simultaneously on the echocardiograph, which has a repetition rate of 1–2 kHz, and printed on paper using thermo-strip chart recorder (HP77510A) at a speed of 10 cm/s as shown in Figure 1. The data were transferred from the hard copy to a computer using a digitizing table and a special mouse (Genetiser GT-1212B). The software transforms the movement of the mouse into digital coordinates; converting the spatial resolution into an effective sampling rate of 125 samples/s. One heartbeat

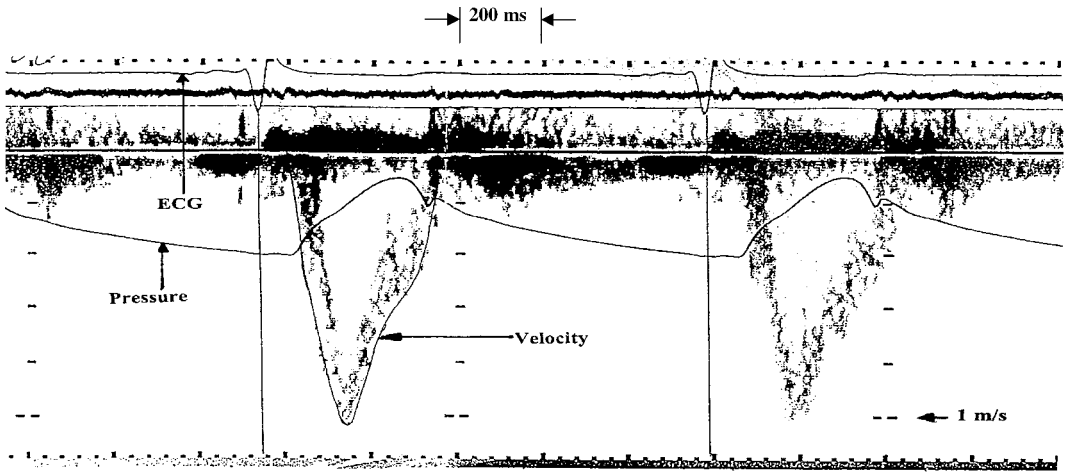

Figure 1 Typical pressure and velocity signals measured in the ascending aorta of a patient undergoing vascular surgery

The noise of the Doppler signal and the outer envelope, which is drawn by hand in the left beat indicating the velocity, are shown. The long vertical lines indicate the peaks of the R-wave of the ECG, which were used as the reference points for the start and end of the beat. The horizontal ticks (abscissa) at top and bottom are time intervals and each indicates a time increment of 200 ms. The vertical ticks (ordinate) indicate velocity and each indicates an increment of 20 cm/s, with a marker for 1 m/s.

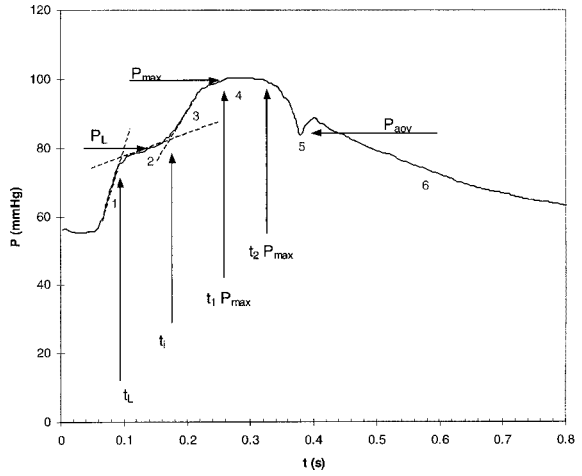

Figure 2 A pressure waveform typical of a group of elderly patients, age 70 ± 5 years, undergoing peripheral vascular surgery showing the characteristic times and pressures analysed in this study

The broken lines are the extrapolations of the linear parts of the curve to determine the t_L, time of the start of the landing, and t_i, the time of the pressure inflection point (see the Methods section and Table 1 for details).

was selected from the pressure and velocity traces at each stage; immediately before, during clamping and as soon as possible following unclamping. The peak of the R-wave on the ECG was taken as time zero. Beats were selected on the basis of clarity, in order to have high resolution for the digitizing process, and regularity, a beat falling within three or more beats of similar shape. Using these criteria we avoided analysing beats that were distorted by catheter displacement or temporary electrical noise in the operating theatre.

Pressure and velocity derivatives are necessary for the calculation of the wave intensity [7]. Although the digitized data were relatively noise free, derivatives inherently magnify noise and some filtering was necessary. Therefore, a seven-point second-order Savitsky and Golay filter was used [8]. This filter fits a least-squares polynomial to the data locally, three points on either side of the current datum, and outputs the slope of the fitted polynomial. The coefficients for this filter are (0.035714, 0.071429, 0.107143, 0.0, −0.107143, −0.071429 and −0.035714).

To test the effect of clamping, we compared the results obtained before clamping with those obtained during clamping and after unclamping. All comparisons were made using paired Students's t tests, and $P < 0.05$ was considered to be statistically significant.

Pressure waveform

The pressure waveform recorded in the ascending aorta of the patients consisted of six distinctive features (numbered 1–6 in Figure 2). (1) The time during early systole when the pressure increases rapidly. (2) The time where the pressure is relatively constant, which we identify as the 'landing'. This is common in the elderly and it has been ascribed to increased stiffness of the arterial tree. The time of the onset of the landing, t_L, is identified as the crossing of the extrapolation of the landing (2) and the initial pressure upstroke (1). (3) The second rapid rise in pressure, the onset of which is determined as the crossing point, usually called the inflection point, of the extrapolation of the landing (2) and second pressure rise (3). Although, the landing is not usually observed in young healthy individuals, an inflection point can often be detected. (4) Maximum pressure in these patients occurred over several sampling points rather than a single maximum point. The ratio of the difference between maximum pressure and the pressure at the inflection point to the maximum pressure is called the 'augmentation index' [9,10]. (5) The dicrotic notch or 'incisura' is associated with the reversal of flow direction in the ascending aorta that starts immediately before the aortic valve closes. (6) The fall of pressure in the aorta during diastole. A summary of the measurements and explanations of the methods used for determining them is given in Table 1.

Analysis

Wave-intensity analysis is a time domain analysis, based on the method of characteristics [7]. Wave intensity, dI, is defined as:

$$\mathrm{d}I = \mathrm{d}P\mathrm{d}U \quad (1)$$

where dP and dU are the change in pressure and velocity over one sampling time respectively. The separation of pressure and velocity into their forward and backward waves requires knowledge of the wave speed, which can be determined from the initial slope of the PU-loop (pressure–velocity loop) [11,12]. The water-hammer equation for the forward waves, P_+, is:

$$\mathrm{d}P_+ = \rho c \mathrm{d}U_+ \quad (2)$$

where ρ is the density of the blood, which is assumed to be 1000 kg/m^3, and c is the wave speed. During the periods when there are no backward waves, P_-, e.g. at the earliest part of systole, it is most likely that forward waves in the ascending aorta are the only waves, since it is too early for the arrival of reflected waves. During that time, eqn (2) indicates that there should be a linear relationship between the change in pressure and the change in velocity. Thus if we plot the measured pressure against the measured velocity over the cardiac cycle we obtain a PU-loop, whose slope during the very early part of systole equals ρc. Figure 3 shows a typical PU-loop for a patient before clamping. The slope of the initial segment of the loop in this case equals $\mathrm{d}P/\mathrm{d}U = 3900\ \mathrm{kPa \cdot s \cdot m^{-1}}$, and corresponds to a wave speed of 3.9 m/s.

By using the wave-intensity analysis and an appro-

Table 1 Notation with an explanation of the methods used for determining the different haemodynamic parameters

Notation	Definition	Method of determination
t_L	Time of the start of the landing	Intersection of extrapolation of the first pressure rise and the landing
t_i	Time of the pressure inflection point	Point of intersection of the extrapolation of the landing and the second pressure rise
P_L	Mean pressure of the landing	$\frac{1}{2}$(pressure at t_L + pressure at t_i)
P_{max}	Maximum pressure	Value of the highest points on the pressure waveform*
tP_{max}	Time of the beginning of the maximum pressure arch	Time when the pressure waveform reaches its peak
U_{max}	Maximum velocity	Value of the highest points on the velocity waveform
tU_{max}	Time of the start of the maximum velocity	Time when the velocity waveform reaches the slope of zero at its peak
t_{RW}	Time of onset of the first reflected wave	Time at which the reflected wave becomes non-zero
tt_{RW}	Duration of the reflected wave	Time duration from the reflected wave becoming non-zero, t_{RW}, in mid-systole until it becomes zero again, in late systole

* It was noticed that in most patients, maximum pressure was not one point as the term 'maximum' suggests. It was found that the maximum occurred over a period of time. The start of that period was pointed to with tP_{max}.

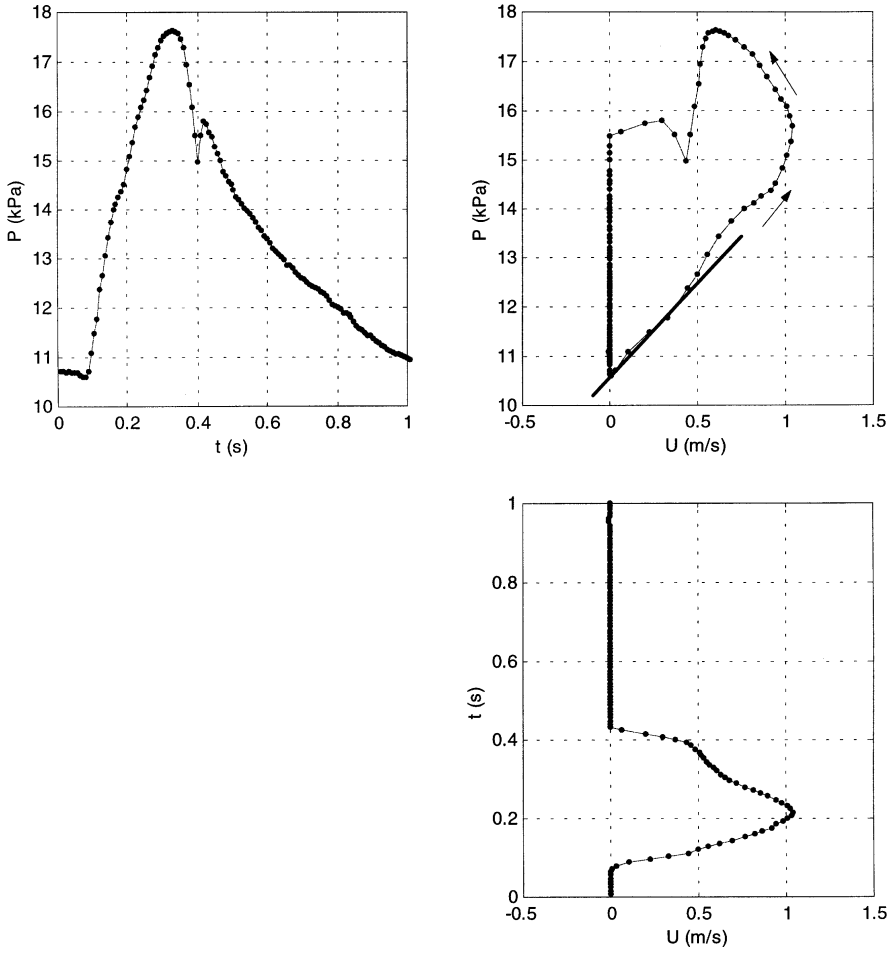

Figure 3 PU-loop

Top right panel: the PU-loop measured in the ascending aorta of a typical patient before clamping. The initial part of the loop is linear and corresponds to a wave speed, c, of 3.9 m/s. The arrows show the direction of the loop and the time interval between dots (sampling points) is 8 ms. The time is implicit in the loop, but apparent on the abscissa of the left panel, which shows the pressure waveform, and the ordinate of the bottom panel, which shows the velocity waveform.

priate estimation of the wave speed, it is possible to separate the forward and backward waves [13]. The pressure and velocity differences across the forward and backward waves are:

$$dP_{\pm} = \frac{1}{2}(dP \pm \rho c dU) \quad (3)$$

$$dU_{\pm} = \frac{1}{2}[dU \pm (dP/\rho c)] \quad (4)$$

The wave intensities of the separated forward and backward waves are:

$$dI_{\pm} = \pm[1/(4\rho c)](dP \pm \rho c dU)^2 \quad (5)$$

We calculated the energy carried by the reflected wave, I_-, by integrating dI_- over the duration of the wave in systole.

The forward and backward pressure waveforms are obtained by integrating dP_+ and dP_-:

$$P_+(t) = P_0 + \sum_{t=0}^{T} dP_+(t)$$
$$P_-(t) = \sum_{t=0}^{T} dP_-(t) \quad (6)$$

where P_0 is the diastolic pressure. The forward and backward velocity waves are obtained by integrating the calculated values of dU_+ and dU_-:

$$U_{\pm}(t) = \sum_{t=0}^{T} dU_{\pm}(t) \quad (7)$$

The hydraulic work per unit area of the aorta done by the heart, W, is calculated as:

$$W = \int_0^T PU dt \quad (8)$$

where T denotes the duration of the cardiac cycle.

RESULTS

The means ± S.D. of the haemodynamic parameters measured before, during clamping and after unclamping are shown in Table 2.

Separation and timings of waves

Figure 4 shows the separation of the measured pressure and velocity into the forward and backward components for a typical beat before clamping. The measured pressure and velocity waves are identical to the forward waves until the onset of the reflected wave. The measured pressure then increases due to the addition of the forward and backward waves, and the measured velocity decreases due to the subtraction of the forward and backward waves.

Table 2 Details of the measurements and calculated parameters on data recorded in patients with peripheral vascular disease before, during clamping and after unclamping

Zero time is taken from the peak of the R-wave of the ECG. Values are their means ± S.D. *, $P < 0.05$, significant difference compared with before clamping.

Variable	Before clamping	During clamping	After unclamping
t_L (ms)	140 ± 20	120 ± 30*	120 ± 10
t_i (ms)	170 ± 20	150 ± 30*	160 ± 30
P_L (mmHg)	96.3 ± 23.09	91.7 ± 18.5	90.2 ± 21.4
P_{max} (mmHg)	115.8 ± 23.20	110 ± 14.7	113.5 ± 25.5
tP_{max} (ms)	260 ± 60	260 ± 50	270 ± 60
U_{max} (cm/s)	103 ± 14.5	104.4 ± 17.7	105.3 ± 23.6
tU_{max} (ms)	180 ± 30	160 ± 30*	170 ± 40
t_{RW} (ms)	160 ± 40	130 ± 30*	150 ± 40
tt_{RW} (ms)	120 ± 30	150 ± 50*	115 ± 28
c (m/s)	3.4 ± 0.3	4.5 ± 1.1*	3.3 ± 0.9
I_- (W/m^2)	4.2 ± 2.2	5.0 ± 2.0*	4.0 ± 1.9
W (W/m^2)	223 ± 80	285 ± 119*	235 ± 90

The time of the pressure inflection point, t_i, correlated with the time of maximum velocity, tU_{max}, ($r = 0.91$), Figure 5(a) and with the onset of the reflected waves, t_{RW}, ($r = 0.87$), Figure 5(b).

Effect of clamping on wave speed

The wave speed, c, increased significantly during clamping compared with its value before clamping (4.5 ± 1.1 m/s versus 3.4 ± 0.3 m/s, $P < 0.05$). The values of wave speed after unclamping were not significantly different from those measured before clamping (3.3 ± 0.9 m/s versus 3.4 ± 0.3 m/s)

Effect of clamping on reflected waves

The magnitude of the reflected wave did not alter with clamping. However, the onset of the reflected wave, t_{RW}, became significantly earlier during clamping compared with the corresponding times before clamping (130 ± 40 ms versus 160 ± 50 ms, $P < 0.05$) (Figure 6). In the patients where the data were recorded several times during clamping, we found that the longer the clamping time, the earlier became the onset of the reflected waves as seen in Figure 7. Although the peak of the reflected wave did not increase during clamping, its duration, tt_{RW}, became significantly longer (150 ± 50 ms versus 120 ± 30 ms, $P < 0.05$). Table 2 includes mean values of the duration of the reflected wave before, during clamping and following unclamping.

The energy carried by the reflected wave, I_-, increased significantly during clamping compared with before clamping (5 ± 2 W/m^2 versus 4.2 ± 2.2 W/m^2). Figure

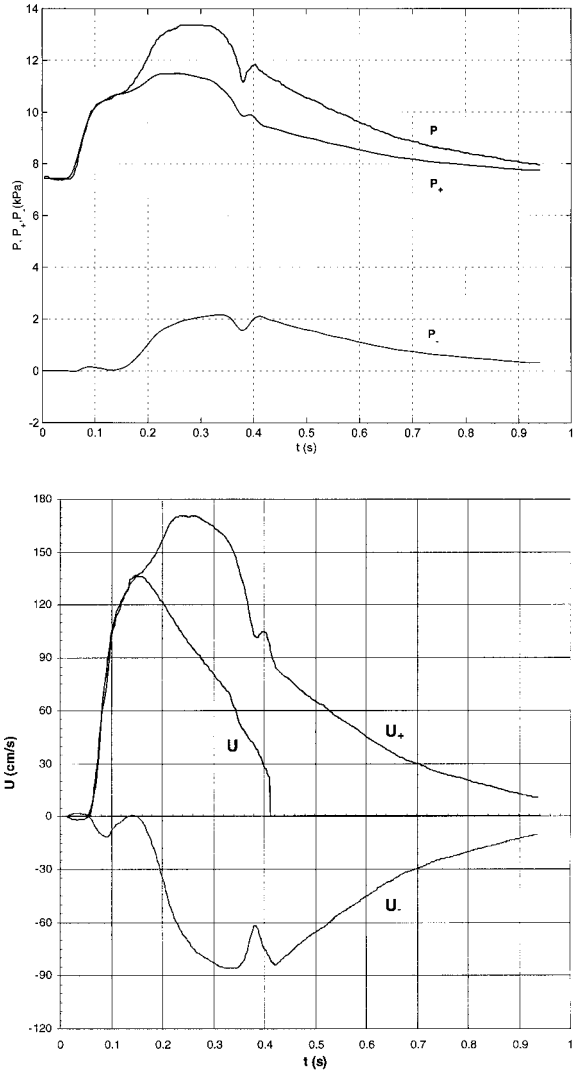

Figure 4 Separation of the pressure and velocity waveforms

Top panel: the measured pressure waveform (P) with its forward (P_+) and backward (P_-) components. The measured pressure equals the sum of the forward and the backward pressure waves. Bottom panel: the measured velocity waveform (U) with its forward (U_+) and backward (U_-) components. The measured velocity equals the subtraction of the backward and the forward velocity waves.

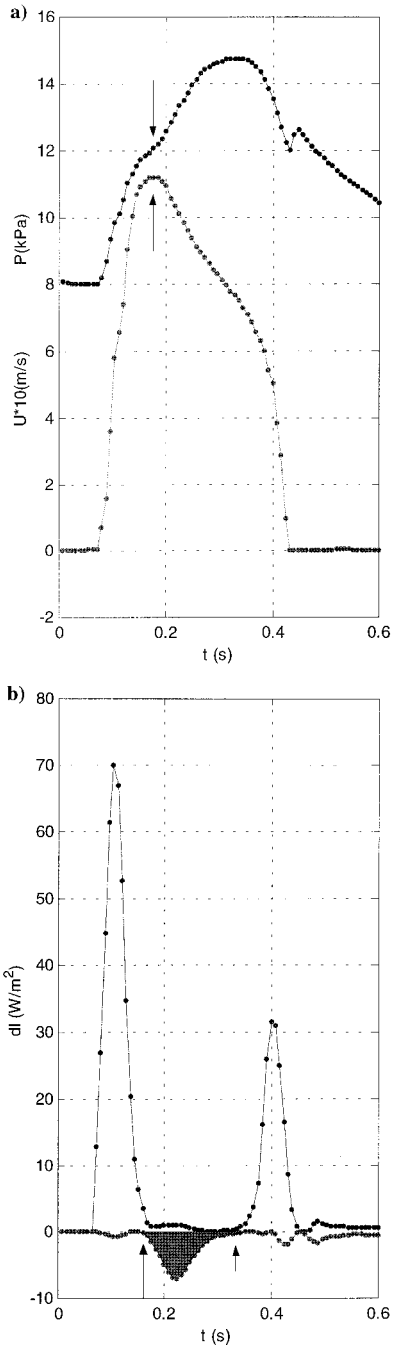

Figure 5 Measured pressure and velocity (a) and calculated wave intensity (b) in the ascending aorta of a typical patient with peripheral vascular disease

The arrows point to the pressure inflection point and the maximum velocity in (a), and to the onset (long arrow) and end, (short arrow) of the reflected wave arriving back at the ascending aorta during systole in (b). The times of the pressure inflection point, maximum velocity and onset of the reflected wave are concurrent.

5(b) shows the integrated area indicating the energy/unit area carried by the reflected wave during systole.

Effect of clamping on hydraulic work

The hydraulic work, W, in our patients increased slightly (271 ± 110 W/m^2 versus 235 ± 79 W/m^2) during clamping, but the increase was not significant. It was observed, however, that systolic pressure fell during clamping in two of the patients and that hydraulic work in those two patients decreased, whereas it increased in all other patients. Pre-operative echcardiographic assessment of LV function of those two patients was poor (ejection fraction $< 20\%$). When we excluded the data of these two patients, the hydraulic work increased significantly by 27% during clamping compared with before clamping (285 ± 119 W/m^2 versus 223 ± 80 W/m^2, $P < 0.05$).

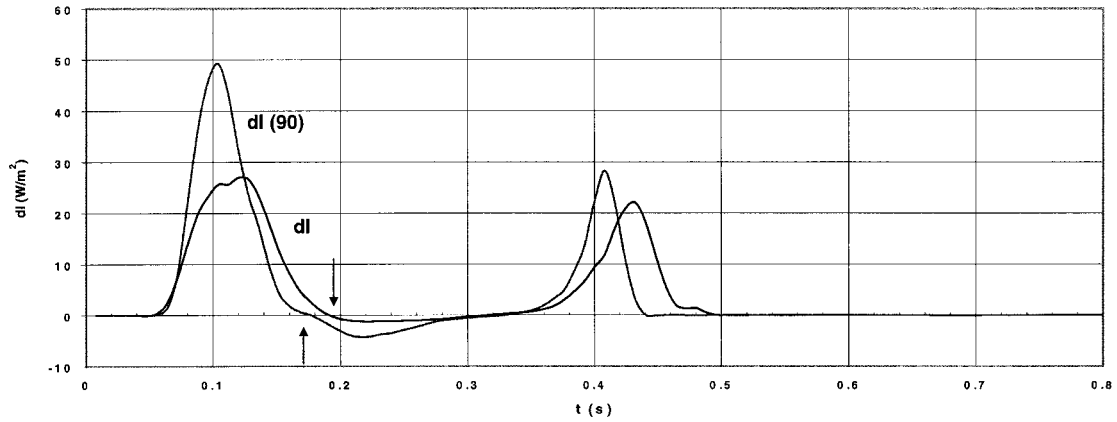

Figure 6 Effect of clamping on the onset of reflected waves

The onset of reflected waves occurs (20 ms) earlier during clamping than before clamping. d*I* is the wave intensity before clamping, and d*I*(90) is the wave intensity 90 min after the clamp has been applied.

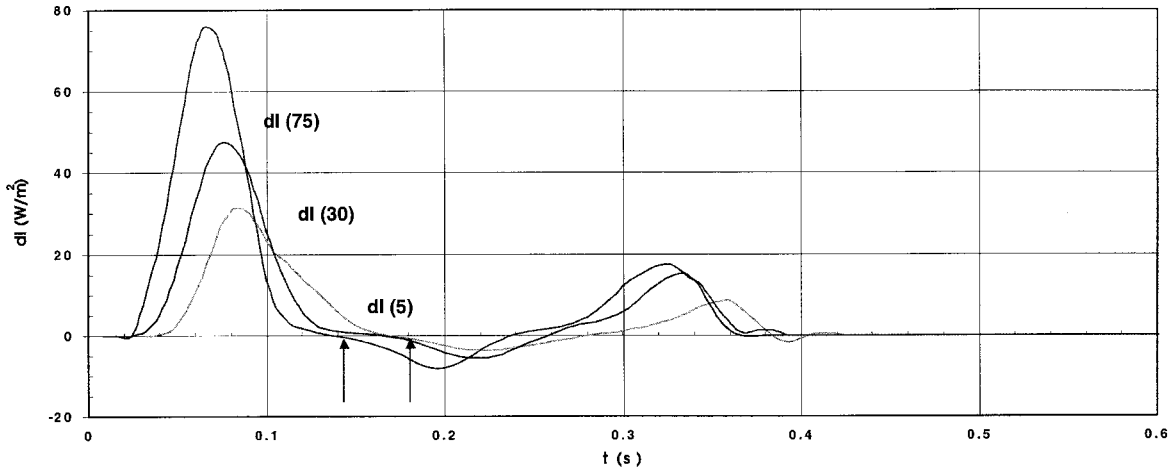

Figure 7 Effect of the duration of clamping on the wave intensity

The longer the clamping time, the earlier the onset of the reflected waves. In this patient the wave intensity starts 20 ms later after 75 min of clamping than after 5 min. Measurements in this patient were taken 5 min [dI(5)], 30 min [dI(30)] and 75 min [dI(75)] after the clamp was applied.

DISCUSSION

Aortic flow velocities in our patients were measured by Doppler ultrasound. This was done by accessing the aortic root, either trans-thoracically from the cardiac apex, underneath the operative sheaths, or using a trans-oesophageal approach. In both cases, even with a good Doppler signal, it was difficult to ascertain exactly when the blood starts and stops (Figure 1). Although there is still no general agreement on whether the inner or the outer edge of the Doppler signal should be used for measuring the times of the flow, Li et al. [14] reported that mean velocity can be estimated to within 5% from the time-averaged maximum Doppler shift. Therefore a subjective choice was made before digitizing the data to consider the outer leading edge as the onset of flow and, even if digitizing the outer edge may have over estimated the actual mean velocity, it would not have affected the velocity differences needed to calculate the wave intensity.

Animal experiments confirm that aortic clamping results in an increase of flow through the upper part of the body and a significant increase in aortic pressure during clamping [15,16]. However, with patients undergoing surgery, pressure is monitored and kept within certain limits pharmacologically. Therefore it was impossible to measure the direct effect of clamping on the arterial pressure.

Wave-intensity analysis makes it possible to separate the pressure and velocity measured in the aortic root into their forward and backward waves. In separating the forward and backward velocity waves, a dicrotic notch appeared on the forward-running velocity, waveform dU_+. This is because the separated forward pressure and

velocity waveforms are identical in shape with a scaling factor of ρc according to the water-hammer equation [eqn (2)].

The waves in both the forward and backward directions establish the measured pressure and velocity waveforms. The strong correlation in time between onset of the reflected wave, maximum velocity and pressure inflection point, suggests that the inflection point on the pressure waveform and the onset of decline on the velocity waveform are due to the reflected waves. The heart generates a pulse wave during systole, which travels downstream until it is reflected, generally from a multiplicity of sites. During the time from the first upstroke of pressure (from the foot of the waveform) to the time of the inflection point, the measured velocity and pressure are identical to that of their forward-running waves, as seen in Figure 4. When the reflected waves return to the aortic root, the measured pressure and velocity waveforms start to deviate from their forward waveforms. The arrival of the reflected compression wave to the measurement site increases the measured pressure as it adds to the measured forward compression pressure wave, and decreases the velocity as it subtracts from the measured velocity wave. The prominence of the landing in elderly people is compatible with increased stiffness of the arteries due to ageing [17], which increases the wave speed. Note that the separated forward pressure waveform of this group of patients does not show a landing making them qualitatively similar to the pressure waveforms of young healthy individuals, which do not usually show a landing.

The calculated hydraulic work per unit area of aorta increased significantly during clamping above resting values. Although this work was calculated at the aortic root, we believe that it should reflect the systolic work of the LV since it was measured in systole, when the aortic valve was open and the aortic root in direct contact with the LV cavity. Since these patients had undergone a routine pre-operative echocardiography assessment to evaluate their ventricular performance and valve operation, and none of them were found to have a valvular disease or malfunction, it was reasonable to assume that there would not be a significant pressure drop across the aortic valve. We believe that the pressure measured at the ascending aorta during systole in these patients should be very close to that of their LV. Similarly, except for the negligble systolic flow to the coronary arteries, the flow in the ascending aorta is equal to that ejected by the LV. Thus the hydraulic work calculated using ascending aortic pressure and velocity should be a fair representation of the LV systolic hydraulic work.

The magnitude of the reflected wave unexpectedly did not alter with clamping. However, its earlier arrival and the longer duration during clamping were significant, which resulted in an increase in the amount of energy carried by the reflected wave. We believe that it is these changes that may influence cardiac function [18]. The increase of both afterload and hydraulic work is likely to have caused an increase in LV oxygen consumption, as has been demonstrated experimentally in animals [19]. This increased demand of oxygen was met by an increased supply of coronary flow in healthy dogs [11], but if this demand cannot be met in patients with coronary artery disease, myocardial ischaemia may be provoked, with all its negative consequences on the LV. The performance of myocardial segments already ischaemic under clamping conditions will deteriorate further during and after surgery.

Study limitations

The number of patients studied was small. However, the findings are consistent in all patients apart from the lack of change in hydraulic work with clamping in the group of patients as a whole. However, when the two patients with a poor ejection fraction were excluded, hydraulic work per unit area of aorta increased significantly.

To reduce the level of subjectivity in choosing the individual beats to be analysed, we tried ensemble averaging the data of three consecutive beats for each patient at each stage of the operation. However, we observed that important features such as the dicrotic notch disappeared with ensemble averaging, and so we resorted to analysing a single typical beat.

The trans-oesophageal approach to the ascending aorta was not accessible in two of the patients in whom data were obtained by the trans-thoracic approach. We do not think that this technical difference should have affected the results. Data collected by both approaches are generally considered of the same quality, and since the site where we recorded aortic velocity was the same in both cases, the measured aortic velocity would be the same in either approach.

Ideally we would like to have measured LV pressures and volume, and calculated its hydraulic work. This would have required special ethics approval since peripheral vascular surgery does not usually involve instrumentation for the heart.

Conclusions

We conclude that the relationship between aortic pressure, velocity and reflected waves is a physiological association, and that waves in the forward and the backward directions establish the measured waves. A significant increase in the wave speed during clamping resulted in the earlier arrival and longer duration of reflected waves. The increased amount of energy carried by the reflected wave suggests an increase in the afterload and the calculated hydraulic work in the ascending aorta suggests an increase in LV hydraulic work during clamping. The increase of afterload and LV hydraulic work during clamping is likely to increase LV oxygen consumption demands. If this demand is not met by

increased coronary artery flow, myocardial ischaemia may be provoked, or aggravated if already present. The resulting deterioration in LV function may contribute to the increased morbidity and mortality of the operation.

REFERENCES

1 Golden, M. A., Donaldson, M. C., Whittemore, A. D. and Mannick, J. A. (1991) Evolving experience with thoracoabdominal aortic aneurism repair at a single institution. J. Vasc. Surg. **13**, 792–797
2 Cox, G. S., O'Hara, P. J., Hertzer, N. R., Piedmonte, M. R., Krajewski, L. P. and Beven, E. G. (1992) Thoracoabdominal aneurism repair: a representative experience. J. Vasc. Surg. **15**, 780–788
3 Svensson, L. G., Crawford, E. S., Hess, K. R., Coselli, J. S. and Safi, H. J. (1993) Experience with 1509 patients undergoing thoracoabdominal aortic operations. J. Vasc. Surg. **17**, 357–370
4 Crawford, E., Bombereger, R., Glaeser, D., Saleh, A. and Russel, W. (1981) Aortoiliac occlusive disease. Factors influencing survival and function following reconstruction operation over a twenty year period. Surgery **90**, 1055–1067
5 Leppo, J., Plaja, J., Gionet, M., Tumolo, J., Paraskos, J. A. and Cutler, B. S. (1987) Non-invasive evaluation of cardiac risk before elective vascular surgery. J. Am. Coll. Cardiol. **9**, 269–276
6 Henein, M. Y., Das, S., O'Sullivan, C., Kakkar, V., Gillbe, C. and Gibson, D. G. (1996) Effect of acute alterations in afterload on left ventricle function in patients with combined coronary artery and peripheral vascular disease. Heart **75**, 151–158
7 Parker, K. H. and Jones, C. J. H. (1990) Forward and backward running waves in the arteries: analysis using the method of characteristics. J. Biomech. Eng. **112**, 322–326
8 Savitsky, A. and Golay, M. J. E. (1964) Smoothing and differentiation of data by simplified least squares procedures. Anal. Chem. **36**, 1627–1639
9 Kelly, R., Hayward, C., Avolio, A. P. and O'Rourke, M. F. (1989) Non-invasive determination of age-related changes in the human arterial pulse. Circulation **80**, 1652–1659
10 Koh, T. W., Pepper, J., DeSouza, A. C. and Parker, K. H. (1998) Analysis of wave reflections in the arterial system using wave intensity: a novel method for predicting the timing and the amplitude of reflected waves. Heart Vessels **13**, 103–113
11 Khir, A. W. (1999) The hemodynamic effects of aortic clamping (PhD thesis). University of London, London
12 Khir, A. W., O'Brien, A., Gibbs, J. S. R. and Parker, K. H. (2001) Determination of wave speed and wave separation in the arteries. J. Biomech. **34**, 1145–1155
13 Parker, K. H., Jones, C. J. H., Dawson, J. R. and Gibson, D. G. (1988) What stops the flow of blood from the heart? Heart Vessels **4**, 241–245
14 Li, S., Hoskins, P. R., Anderson, T. and McDicken, W. N. (1993) Measurement of mean velocity during pulsatile flow using time-averaged maximum frequency of Doppler ultrasound waveforms. Ultrasound Med. Biol. **19**, 105–113
15 Barcroft, H. (1933) Observations on the pumping action of the heart. J. Physiol. (London) **78**, 186–195
16 Barcroft, H. and Samaan, A. (1935) The explanation of the increase in systemic flow caused by occluding the descending thoracic aorta. J. Physiol. (London) **85**, 47–61
17 Avolio, A. P., Fa-Qua, D., Wei-Qiang, L., Yoo-Fei, L., Zhen-Dong, H., Lian-Fen, X. and O'Rourke, M. F. (1985) Effects of aging on arterial distensibility in populations with high and low prevalance of hypertension: comparison between urban and rural communities in China. Circulation **71**, 202–210
18 Kirkpatrick, R. D., Campbell, K. B., Bell, D. L. and Taheri, H. (1991) Method for studying arterial wave transmission effects on left ventricular function. Am. J. Physiol. **260**, H1003–H1012
19 Kelly, R. P., Tunin, R. and Kass, D. A. (1992) Effect of reduced aortic compliance on cardiac efficiency and contractile function of in situ canine left ventricle. Circ. Res. **71**, 490–501

Received 6 February 2001/4 July 2001; accepted 29 August 2001